The International Journal of Pavement Engineering, Vol. 2, pp. 187–199
Reprints available directly from the publisher
Photocopying permitted by license only

Non-linear Finite-Element Analysis to Predict Permanent Deformations in Pavement Structures Under Moving Loads

WEIXIN SHEN[a]* and DAVID J. KIRKNER[b]

[a]*JAYCOR Inc., 3394 Carmel Mountain Road, San Diego, CA 92121, USA;* [b]*Department of Civil Engineering and Geological Sciences, University of Notre Dame, Notre Dame, IN 46556, USA*

(Received 20 September 2000; In final form 19 February 2001)

The structural analysis of pavement systems is quite a difficult problem; it involves a layered medium, usually modeled as unbounded in extent, subjected to moving loads. A principle concern is the permanent deformation remaining when the load exceeds design values; the so-called rutting phenomenon. A steady, moving load, assumed quasi-static, can be handled by employing a moving coordinate system to advantage; in essence converting the modeling problem to one with a stationary load. However, the unbounded domain is still problematical. The common practice of using rollers on the boundaries of a truncated domain will lead to a loss of accuracy, especially for points near the truncated boundaries. In a finite element approach to the steady-state problem in which a load moves at a constant speed on an elastic–plastic layered system "boundary effects" due to the inherent nonlinear boundary conditions are so obvious that it is almost impossible to evaluate residual displacements. In this paper, a method is proposed to treat the involved, nonlinear boundary conditions and to allow accurate prediction of the residual displacements. A modified iterative scheme is constructed and infinite elements are employed to treat the unbounded domain. The infinite element formulation involves the residual displacements and, therefore, must be used together with the modified iterative scheme. Numerical results indicate that the adoption of the infinite elements together with the modified iterative scheme completely eliminate the "boundary effects" and greatly improve the accuracy of calculated residual displacements.

Keywords: Moving load; Nonlinear boundary condition; Infinite elements; Pavement

1. INTRODUCTION

Usually, the response of a flexible pavement to moving loads is predicted from an elastic multilayer analysis. This type of analysis is based on the fact that the response of pavements to moving loads and stationary loads are the same if a moving coordinate system is used in the moving load case (if the moving

*Corresponding author. E-mail: wshen@jaycor.com

loads are assumed quasi-static) and if the paving and subgrade materials are linear elastic. The structural failure of pavements is usually related by empirical equations to the stresses or strains predicted from an elastic analysis. For example, rutting is usually related to vertical strains or stresses on the top of the subgrade, while fatigue is related to the tensile stresses on the bottom of the asphalt concrete layer. The theoretical inconsistency is quite obvious. Degradation of pavement structures due to the accumulated effects of inelastic strain cannot be accurately modeled from a linear elastic analysis. In reality, asphalt mixtures are viscoelastic materials, and base and subgrade materials exhibit plasticity. So, it is not surprising that the difference between predicted and actual pavement response is usually large.

Much research has been done recently on using the finite element method to predict pavement response, wherein it is possible to take into account such complicating factors as dynamic loading and nonlinear constitutive laws for material behavior. Two-dimensional nonlinear and/or dynamic analysis is now common. Three-dimensional nonlinear analysis of a multi-layered halfspace has also been performed (Desai and Siriwardane, 1982; Siriwardane and Desai, 1983; Forte *et al.*, 1992; Ioannides and Donnelly, 1992; Kokkins, 1992). However, none of these methods treat moving loads. Zaghloul and White (1993) dealt with moving loads by translating the contact areas between the loads and the pavement surface on the finite element mesh and solving the resulting transient problem. Since the loads are moving on the mesh and the distances between the loads and the mesh boundaries must be large enough to overcome the errors introduced in truncating the infinite domain, the finite element mesh must be very large in this method to get accurate results.

For steady, moving loads a moving coordinate system can be used to advantage. This approach was used by Lynch (1969), Bapat and Batra (1984) and Bhargava *et al.* (1985) in solving roller problems. Dang Van and Maitournam (1993) and Kirkner *et al.* (1994; 1996) proposed a finite element algorithm for predicting the permanent deformation and residual stress state with each pass of moving loads on a layered elastic–plastic halfspace. The moving coordinate can be viewed either as a time variable or as a space variable, which means the displacements far behind the loads are also the displacements when the loads have long passed and are the permanent deformations. This suggests that the displacements far behind the loads should not change along the coordinate in the moving-load direction. This approach requires a relatively small amount of storage and is numerically easy to implement. In addition, complicated material constitutive relationships can be included conveniently.

Since pavements and their supporting structure are modeled as infinite in length and thickness, the treatment of the unbounded domain is an important aspect in every finite element program to analyze pavement responses. The previously mentioned methods truncate the domain and employ rollers on the truncated boundaries. This is based on the assumption that as long as the truncated domain is large enough, the errors introduced are insignificant. This treatment usually increases the stiffness of the pavement structure and leads to smaller calculated displacements than actual values, especially for points near the truncated boundaries. In some problems where only the displacements and stresses near the load are of interest, the error due to the boundary effects is acceptable when a reasonably large mesh is used. However, for problems involving multiple loads with relatively large distances between them, or a high load which will lead to significant yielding, the costs of storage and computing time may be significant.

It should also be noted that if the base and/or sub-base supporting the pavement are elastic–plastic, displacements far behind the loads eventually reach some finite non-zero values (the permanent deformation or "rut" profile). Thus, the boundary conditions far behind the loads at infinity are nonlinear. Whether truncating the domain and imposing rollers can successfully treat the non-linear boundary conditions is questionable. Numerical experiments have shown large errors near the truncated boundaries.

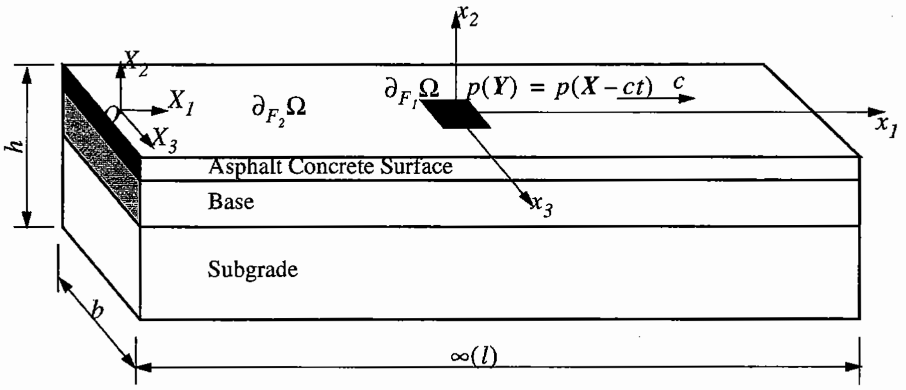

FIGURE 1 Multi-layered flexible pavement system subjected to a moving load.

In this paper, a method will be proposed for calculating the residual displacement which offers some computational advantage. A modified iterative scheme can be constructed to treat the nonlinear boundary conditions. In addition, infinite elements will be introduced into the finite element algorithm to treat the infinite domain. Infinite element formulations also involve the prediction of the residual displacements during each iteration, and therefore, the modified iterative affects the infinite element formulation. Results for a finite element analysis using the traditional roller boundary conditions and infinite elements will be given for comparison.

2. PROBLEM DESCRIPTION

Figure 1 shows a typical multi-layered flexible pavement system. The layered system is homogenous in the horizontal directions and infinite in extent and has a total thickness of h. Materials in the system are considered elastic–plastic. **X** denotes the fixed coordinate system (O, X_1, X_2, X_3). Let Ω, $\partial\Omega$, $\partial_{F_1}\Omega(t)$, and $\partial_{F_2}\Omega(t)$ denote the layered elastic–plastic domain, the pavement surface, the loaded part of the surface, and the unloaded part of the surface, respectively. They are defined as

$$\Omega = \{(X_1, X_2, X_3) | -\infty < X_1 < \infty, 0 < X_2 < h, -\infty < X_3 < \infty\} \tag{1a}$$

$$\partial\Omega = \{(X_1, 0, X_3) | -\infty < X_1 < \infty, -\infty < X_3 < \infty\} \tag{1b}$$

$$\partial_{F_1}\Omega(t) = \{(X_1, 0, X_3) | -l_1 + ct \leq X_1 \leq l_1 + ct, -l_3 \leq X_3 \leq l_3\} \tag{1c}$$

$$\partial_{F_2}\Omega(t) = \partial\Omega - \partial_{F_1}\Omega(t) \tag{1d}$$

Here, for simplicity, the loaded area is assumed to be a rectangle, $2l_1 \times 2l_3$. Any closed region is easily handled.

A moving coordinate system can be introduced to solve the steady state problem by defining $x_1 = X_1 - ct$, $x_2 = X_2$, and $x_3 = X_3$, and placing the origin at the center of the load. Using the moving coordinate system, time is removed as an explicit variable in the problem. In the moving coordinate system, the loads are applied on fixed geometrical surfaces. For a fixed plane, $X_1 =$ constant, $x_1 = \infty$ indicates the time when loads are applied or a plane far ahead of the load and $x_1 = -\infty$ is the time after loads have long passed or a material plane far behind the load. The two parts of the pavement surface are now independent of time and can be described as

$$\partial_{F_1}\Omega = \{(x_1,0,x_3)| -l_1 \le x_1 \le l_1 - ct, -l_3 \le x_3 \le l_3\} \tag{2a}$$

$$\partial_{F_2}\Omega = \partial\Omega - \partial_{F_1}\Omega \tag{2b}$$

Let $\boldsymbol{U} = \{u_1,u_2,u_3\}^{\mathrm{T}}$ be the displacement vector, $\boldsymbol{\sigma}$, $\mathbf{e}$, $\mathbf{e}^{\mathrm{e}}$ and $\mathbf{e}^{\mathrm{p}}$ the stress, the strain, the elastic strain and the plastic strain tensors, respectively, which are stored as 6×1 vectors, $\boldsymbol{D}$ the fourth order elasticity tensor, characterized by a 6×6 matrix. The field equations and boundary conditions can be listed as

$$\partial^{\mathrm{T}}\boldsymbol{\sigma} = 0 \quad \text{(equilibrium)} \tag{3}$$

$$\mathrm{e} = \partial\mathbf{U} \quad \text{(strain–displacement relationship)} \tag{4}$$

where ∂ is the linear strain–displacement operator matrix.

Inertial forces are neglected in Eq. (3) because the speed of the moving loads is much smaller than the velocities of the stress waves in pavements. The problem is considered quasi-static. However, inertial forces can be easily included in the formulation.

The constitutive law is

$$\boldsymbol{\sigma} = \boldsymbol{D}\mathbf{e}^{e} \tag{5}$$

$$\mathbf{e} = \mathbf{e}^{e} + \mathbf{e}^{p} \tag{6}$$

with associated flow rule and yield criterion expressed as

$$\mathbf{e}^{p}_{,x_1} = \lambda\frac{\partial f}{\partial\boldsymbol{\sigma}} \tag{7}$$

and

$$f(\boldsymbol{\sigma},\kappa) = 0 \tag{8}$$

where κ is the hardening parameter. When no isotropic or kinematic hardening is involved, Eq. (8) can be simplified to

$$f(\boldsymbol{\sigma}) = 0 \tag{9}$$

The boundary conditions on the pavement surface are

$$\text{On}\,\partial_{F_1}\Omega: \quad \sigma_{22}(x_1,0,x_3) = -p(x_1,x_3) \tag{10a}$$

$$\text{On}\,\partial_{F_2}\Omega: \sigma_{22}(x_1,0,x_3) = 0 \tag{10b}$$

$$\text{On}\,\partial\Omega: \sigma_{12} = \sigma_{11} = 0 \tag{10c}$$

where $p(x_1,x_3)$ is the surface pressure applied vertically to $\partial_{F_1}\Omega$.

If the pavement is constructed on a rock foundation, the bottom of the pavement is assumed to be fixed, i.e.

$$\boldsymbol{U}(x_1,-h,x_3) = \mathbf{0} \tag{11a}$$

Other bottom conditions (such as frictionless) can easily be handled.

The conditions at infinity are

$$\boldsymbol{U}(\infty,x_2,x_3) = \mathbf{0} \tag{11b}$$

$$\boldsymbol{U}(-\infty,x_2,x_3) = \boldsymbol{U}^{R}(x_2,x_3) \tag{11c}$$

$$\boldsymbol{U}(x_1,x_2,\pm\infty) = \mathbf{0} \tag{11d}$$

in which, $\boldsymbol{U}^{R}$ is the permanent or residual displacement field remaining after the load has long passed. As such, this is a nonlinear boundary condition.

In addition to these boundary conditions, displacement and stress continuity conditions must also be satisfied on the interfaces between the pavements layers.

3. FINITE ELEMENTS FORMULATION OF THE MOVING LOAD PROBLEM

Notice that the coordinate x_1, may have different physical perspectives. If time is considered as fixed at an instant then the solution to the above boundary value problem, in terms of x_1, x_2, x_3, may be thought of as a "snapshot" of the physical domain (in terms of X_1, X_2, X_3) at an instant. Alternatively, if X_1 is considered to be held fixed then the graph of any quantity (stress, strain, displacement) expressed as a function of x_1 is a time history of that particular quantity. This implies that integration over time is converted, in the moving coordinate system, to integration over space.

In order to evaluate the constitutive relations for an elastic–plastic material, the evolution Eq. (7) for the plastic strain in essence must be integrated. Notice in Eq. (7) that time derivatives of plastic strains have been replaced by derivatives with respect to x in the moving coordinate system. Thus, an integration of the response history in time is equivalent in the moving reference frame to an integration over x_1.

The principle of virtual work for the above boundary value problem in the moving coordinate frame can be expressed as

$$\int_{\Omega} \delta \mathbf{e}^{\mathrm{T}} \boldsymbol{\sigma} \, \mathrm{d}V = -\int_{\partial,\Omega} \delta u_2 p(x_1, x_3) \, \mathrm{d}S \qquad (12)$$

where the admissible displacements are assumed to satisfy the essential boundary conditions. However, as indicated by Eq. (11c), the displacement at minus infinity are residual displacements which are to be found, therefore, the boundary condition at minus infinity is a nonlinear boundary condition.

An iterative strategy based on a simple initial stress method (Bathe, 1996) has been found to work well for this problem. A superscript is used to indicate the iteration number. Thus σm indicates the mth iteration. Let $\Delta\boldsymbol{\sigma} = \sigma^m - \sigma^{m-1}$. Then Eq. (12) may be written

$$\int_{\Omega} \delta \mathbf{e}^{T} \Delta\boldsymbol{\sigma} \, \mathrm{d}V = -\int_{\partial,\Omega} \delta u_2 p(x_1, x_3) \, \mathrm{d}S - \int_{\Omega} \delta \mathbf{e}^{T} \sigma^{m-1} \mathrm{d}V \qquad (13)$$

In the initial stress method, the elastic stress–strain relation (5) are used to relate increments of stresses to increments of strains. Thus, Eq. (13) becomes

$$\int_{\Omega} \delta \mathbf{e}^{T} \boldsymbol{D} \Delta\boldsymbol{\epsilon} \, \mathrm{d}V = -\int_{\partial,\Omega} \delta u_2 p(x_1, x_3) \, \mathrm{d}S - \int_{\Omega} \delta \mathbf{e}^{T} \sigma^{m-1} \, \mathrm{d}V \qquad (14)$$

The displacements may be related to element nodal displacements $\boldsymbol{U}^e$ by a $3 \times 3n$ shape function matrix, $\boldsymbol{N}$, as follows

$$\boldsymbol{U} = \boldsymbol{N}^T \boldsymbol{U}^e \qquad (15)$$

where $\boldsymbol{N}$ contains the finite element shape functions, and where n is the number of nodes. For linear shape functions, used herein, $n = 8$. Using the strain–displacement relation (4) with Eq. (15) yields

$$\mathbf{e} = \boldsymbol{B} \boldsymbol{U}^e \qquad (16)$$

where $\boldsymbol{B} = \partial \boldsymbol{N}^T$ is the discrete strain–displacement matrix. Therefore the element stiffness matrix and load vector are given by

$$\boldsymbol{K}^e = \int_{\Omega^e} \boldsymbol{B}^T \boldsymbol{D} \boldsymbol{B} \, \mathrm{d}V \qquad (17)$$

$$\boldsymbol{p}^{e,m} = -\int_{\partial_{F_1}\Omega^e} \hat{\boldsymbol{N}} p(x_1, x_3) \, \mathrm{d}S - \int_{\Omega^e} \boldsymbol{B}^T \sigma^m \, \mathrm{d}V \qquad (18)$$

where $\boldsymbol{N}$ is a $3n \times 1$ matrix containing the nodal shape functions.

The standard assembly technique then yields the following global equation:

$$\boldsymbol{K} \Delta \boldsymbol{U} = \boldsymbol{P}^m \qquad (19)$$

If the infinite domain is treated by truncating the domain to a length l in the x_1 direction and a width b in the x_3 direction, and imposing roller boundary conditions, the following boundary conditions are used instead of Eqs. (11b)–(11d)

$$u_1\left(\pm\frac{l}{2},x_2,x_3\right)=\sigma_{12}\left(\pm\frac{l}{2},x_2,x_3\right)=\sigma_{13}\left(\pm\frac{l}{2},x_2,x_3\right)=0 \quad (20a)$$

$$u_3(x_1,x_2,\pm b/2)=\sigma_{13}(x_1,x_2,\pm b/2)=\sigma_{23}(x_1,x_2,\pm b/2)=0 \quad (20b)$$

4. RESIDUAL DISPLACEMENT CALCULATIONS

Boundary conditions (20a) and (20b) are approximations to the real boundary conditions (11b)–(11d). In addition to the error due to truncating the domain, the assumption that $u_1(-l/2,x_2,x_3)=0$ is not correct because of the existence of permanent displacements due to plastic deformation. Numerical results have shown significant "boundary effects" (calculated vertical displacements are positive or far from the actual values) near $x_1=-l/2$. Also, the profile of the displacement along the centerline of the pavement far behind the load is not horizontal as expected, instead, it fluctuates near the left truncated boundary. In the moving coordinate system permanent displacements are the displacements far behind the load and are obtained as the displacements near the left boundary. Thus, boundary effects make the evaluation of the permanent displacements difficult. Herein a method is developed for calculating the rut depth and profile, which offers some computational advantage. Using this method, an improved iterative scheme can also be constructed for determining the elastic–plastic moving load solution.

4.1 Expressions for the Residual Displacements

In this section, formulations are derived to show that the residual displacements on the left boundary of the finite element mesh can be estimated from the displacements in the interior part of the finite element mesh and the elastic part of the displacements.

Substituting the constitutive relationship (5) into the virtual work statement of the problem (12) yields

$$\int_{\Omega}\delta\mathbf{e}^T\boldsymbol{D}\boldsymbol{\epsilon}\,\mathrm{d}V=-\int_{\partial_F\Omega}\delta u_2 p(x_1,x_3)\,\mathrm{d}S+\int_{\Omega}\delta\mathbf{e}^T\boldsymbol{D}\mathbf{e}^p\,\mathrm{d}V \quad (21)$$

Alternatively, operating on both sides of the standard additive decomposition of the strain tensor (6) with $\delta\mathbf{e}^{\mathrm{T}}$ and integrating over the domain Ω gives

$$\int_{\Omega}\delta\mathbf{e}^T\boldsymbol{D}\mathbf{e}\,\mathrm{d}V=\int_{\Omega}\delta\mathbf{e}^T\boldsymbol{D}\mathbf{e}^e\,\mathrm{d}V+\int_{\Omega}\delta\mathbf{e}^T\boldsymbol{D}\mathbf{e}^p\,\mathrm{d}V \quad (22)$$

Then subtracting Eq. (22) from Eq. (21) results in

$$\int_{\Omega}\delta\mathbf{e}^T\boldsymbol{D}\mathbf{e}^e\,\mathrm{d}V=-\int_{\partial_{F_1}\Omega}\delta\boldsymbol{U}^T u_2 p(x_1,x_3)\,\mathrm{d}S \quad (23)$$

Equation (23) states that the elastic part of the strain tensor can be thought of as the strains from a related boundary value problem on the same domain — only with an elastic material.

Using Eq. (23), an alternative method can be developed to obtain the residual displacement field, i.e. the displacement field remaining long after the load has passed. This is based on the following assumption: material points are in a state of loading until $x_1=x_1^*(x_2,x_3)$ and subsequently (that is, for $x_1\le x_1^*(x_2,x_3)$) are elastically unloading $x_1^*(x_2,x_3)$ is a limit-transition surface. Points to the left of x_1^* will not encounter any further plastic loading. This means that the components of the plastic strain tensor are constant for points $x_1<x_1^*(x_2,x_3)$.

The strain–displacement relation for the axial strain in the x_1 direction is

$$\epsilon_1=\frac{\partial u_1}{\partial x_1}=\epsilon_1^e+\epsilon_1^p. \quad (24)$$

Since ϵ_1^e can be obtained from the related elastic problem, this can also be written as

$$\epsilon_1^e = \frac{\partial u_1^e}{\partial x_1}. \tag{25}$$

Define x_{1m}^* be the left-most point on the surface $x_1^*(x_2, x_3)$, i.e. $x_{1m}^* = \min(x_1^*(x_2, x_3))$.

Let $(\hat{x}_1, x_2, x_3)$ be an arbitrary point with $\hat{x}_1 \leq x_{1m}^*$. Integrating both sides of Eq. (24) using Eq. (25) yields

$$\begin{aligned} u_1(\hat{x}_1, x_2, x_3) &- u_1(-\infty, x_2, x_3) \\ &= u_1^e(\hat{x}_1, x_2, x_3) - u_1^e(-\infty, x_2, x_3) \\ &\quad + \int_{-\infty}^{x} \epsilon_1^p \, dx_1 \end{aligned} \tag{26}$$

or

$$\begin{aligned} u_1(\hat{x}_1, x_2, x_3) &- u_1^e(\hat{x}_1, x_2, x_3) \\ &= u_1^R(x_2, x_3) + \int_{-\infty}^{x} \epsilon_1^p \, dx_1 \end{aligned} \tag{27}$$

where

$$\begin{aligned} u_1^R(x_2, x_3) &= u_1(-\infty, x_2, x_3) \\ u_1^e(-\infty, x_2, x_3) &= 0. \end{aligned} \tag{28}$$

In Eq. (28) $u_1^R(x_2, x_3)$ is the permanent or residual displacement remaining after the load has long passed. Since ϵ_1^p is constant, in order for u_1^R to be bounded, ϵ_1^p must be zero, i.e. $\epsilon_1^p(x_1, x_2, x_3) = 0$, $x_1 \leq \hat{x} \leq x_1^*$, which is expected physically. Thus Eq. (27) gives a simple expression for calculating the residual u_1 displacement

$$u_1^R(x_2, x_3) = u_1(\hat{x}_1, x_2, x_3) - u_1^e(\hat{x}_1, x_2, x_3) \tag{29}$$

The vertical displacement can be treated as follows:

$$\epsilon_2 = \frac{\partial u_2}{\partial x_2} = \epsilon_2^e + \epsilon_2^p = \frac{\partial u_2^e}{\partial x_2} + \epsilon_2^p \tag{30}$$

Evaluate Eq. (30) at $x_1 = -\infty$ and at $x_1 = \hat{x}$ and subtract the resulting expressions, using the fact that $\mathbf{e}^p$ is not a function of x_1. This yields

$$\begin{aligned} \frac{\partial}{\partial x_2} u_2(-\infty, x_2, x_3) &- \frac{\partial}{\partial x_2} u_2(\hat{x}_1, x_2, x_3) \\ &= \frac{\partial}{\partial x_2} u_2^e(-\infty, x_2, x_3) - \frac{\partial}{\partial x_2} u_2^e(\hat{x}_1, x_2, x_3) \end{aligned} \tag{31}$$

Now integrate Eq. (31) from $-h$ to an arbitrary point x_2 and use the bottom boundary condition of fixity to yield

$$u_2^R(x_2, x_3) = u_2(\hat{x}_1, x_2, x_3) - u_2^e(\hat{x}_1, x_2, x_3) \tag{32}$$

where as above $u_2^R = (x_2, x_3) = u_2(-\infty, x_2, x_3)$. u_3 can be treated in a similar manner to yield

$$u_3^R(x_2, x_3) = u_3(\hat{x}_1, x_2, x_3) - u_3^e(\hat{x}_1, x_2, x_3) \tag{33}$$

The utility of Eqs. (29), (32) and (33) is due to the fact that it is easier to obtain an accurate estimate for the displacements near the load than at $x_1 = -\infty$ because of boundary effects.

4.2 Modified Iterative Scheme

The above is not only useful as a means of obtaining the residual displacement field with a smaller mesh, but also suggests a modification to the iterative scheme which allows the non-linear displacement boundary conditions to be included instead of the roller boundary condition.

The complete statement of the problem defined by Eq. (12) should give the class of functions from which the displacement field is chosen; this means specifying the essential boundary conditions. Since the problem is solved numerically, using a finite element method, this means specifying essential boundary conditions on a domain of finite extent and then, formally, the solution is the limit as the extent is allowed to go to infinity. In practice the results should remain fairly constant in the vicinity of the load and the residual displacements stabilize for a couple of meshes with different extents. For each analysis the domain is truncated and an approximation is used on the boundaries. For elastic problems, zero displacements or stresses are used; often a combination. For example roller boundary conditions

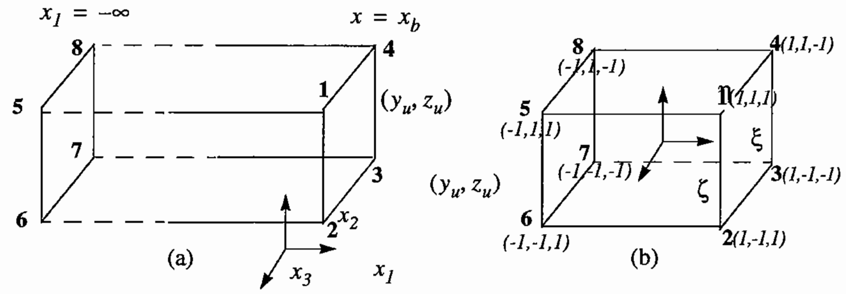

FIGURE 2 Type-1 infinite element.

on the lateral boundaries specify one displacement condition and two shear stress conditions. In the moving load problem the left lateral boundary corresponds to each plane long after the load has passed (for a right-moving load). The results presented above suggest a modified iterative scheme, which should improve the results. The boundary condition on the left lateral boundary will be specified displacements and the value of the displacement will be updated each iteration using the displacements from the last iteration at $x_1 \leq x_1^*$ and the elastic displacements on this same plane. If the assumption on which this calculation is based (material points are in a state of loading until $x_1 = x_1^*$ and subsequently are elastically unloading) is satisfied then the displacement boundary condition should converge to the theoretically correct values. The accuracy of the basic assumption can be monitored during the solution process.

5. INFINITE ELEMENT FORMULATION

Infinite elements are sometimes used in a finite element mesh to simulate an unbounded domain. In this section, element stiffness matrices and equivalent nodal load vectors are reviewed for two kinds of infinite elements. Formulations involve the residual displacements far behind the load, which can be estimated using Eqs. (29), (32) and (33) developed in the previous section.

Two types of infinite elements, as shown in Figs. 2 and 3, are needed for this type of problem. Type-1 infinite element is infinite along one coordinate (x_1 direction is shown in Fig. 2) and the dimension of the cross-section of the element does not change with this coordinate. Type-2 infinite element is infinite along two coordinates (x_1, and x_3 in Fig. 3) and has a constant thickness in the other coordinate.

Standard mapping procedures for infinite elements are employed. The details will be ommitted here. See Zienkiewicz and Taylor (1989) and references therein for a discussion of this topic.

The principle of virtual work can then be written for an infinite element as

$$\left(\delta U_l^e\right)^{\mathrm{T}} K^e U_l^e = \left(\delta U_l^e\right)^{\mathrm{T}} \left(P^e + K^e U_p^e\right) \tag{34}$$

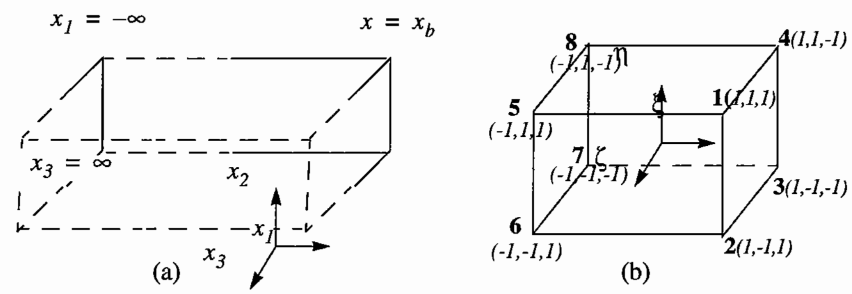

FIGURE 3 Type-2 infinite element.

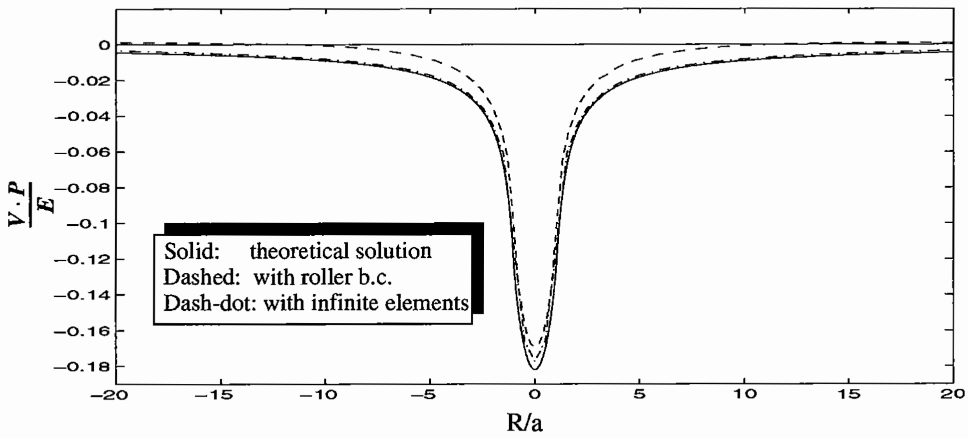

FIGURE 4 Displacement on the surface of an elastic halfspace.

where $\boldsymbol{K}^e$ is the element stiffness matrix, $\boldsymbol{K}^e = \int_e \boldsymbol{B}^{\mathrm{T}}\boldsymbol{D}\boldsymbol{B}\,\mathrm{d}v$;

$\boldsymbol{U}_l^e$ is the element nodal displacement vector on the finite boundary in the x_1 direction

$$\boldsymbol{U}_l^e = \{u_1^1, u_2^1, u_3^1, u_1^2, u_2^2, u_3^2, u_1^3, u_2^3, u_3^3, u_1^4, u_2^4, u_3^4\}^{\mathrm{T}};$$

$\boldsymbol{U}_p^e$ contains the nodal displacements at minus infinity, i.e. the permanent displacement vector

$$\boldsymbol{U}_p^e = \{u_1^5, u_2^5, u_3^5, u_1^6, u_2^6, u_3^6, u_1^7, u_2^7, u_3^7, u_1^8, u_2^8, u_3^8\}^{\mathrm{T}};$$

$\boldsymbol{B}$ is the infinite element strain–displacement matrix;

$\boldsymbol{P}^e$ is the element equivalent nodal load vector.

$\boldsymbol{K}^e$ and $\boldsymbol{P}^e$ can be assembled into the global stiffness matrix and equivalent load vector following the standard assembly procedure. The $\boldsymbol{U}_p^e$ term on the right hand side of Eq. (34) contains the permanent deformations which are unknown. Using the residual displacement calculation, Eqs. (29), (32) and (33), it can be predicted and modified during each iteration.

6. RESULTS

In this section, some numerical results are given using the method developed in the previous sections. First, a

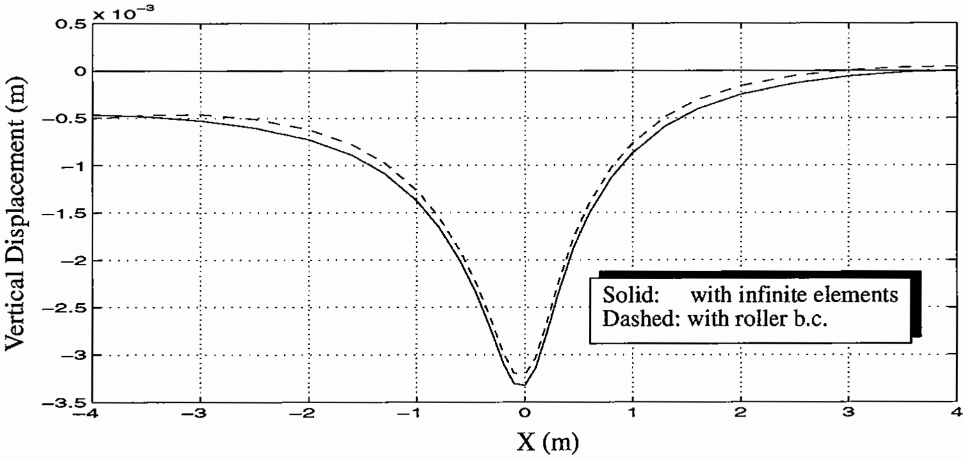

FIGURE 5 Vertical displacement along the centerline of pavement surface.

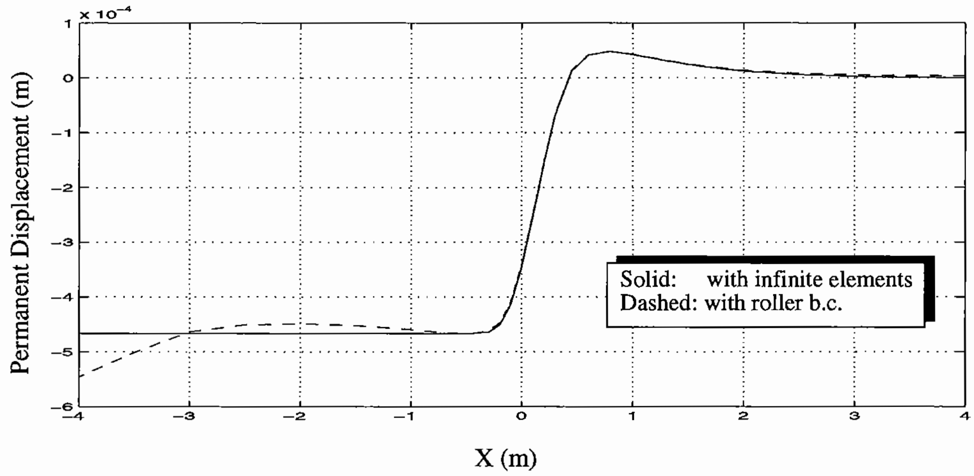

FIGURE 6 Vertical permanent displacement after the load has passed.

standard Boussinesq problem is used to check the utility of the infinite elements. Second, displacement profiles obtained by using roller boundary conditions and the infinite elements with the modified iterative scheme are compared. It is shown that the use of infinite elements can greatly improve the numerical efficiency and make the prediction of permanent displacements much easier.

6.1 Elastic Solution

An elastic halfspace with a uniform circular load P of radius a applied vertically to the top surface is used to check the utility of using infinite elements instead of the roller boundary condition. The elastic modulus of the halfspace is denoted E and Possion's ratio is 0.3. The vertical displacement, V, on the surface of the halfspace is given in Fig. 4, where dimensionless units are used. R is the distance from the calculated point to the center of the load. A total of $40 \times 15 \times 16$ elements are used in the finite element mesh which represents a truncated domain of $20a \times 20a \times 20a$. When roller boundary conditions are used, the vertical displacements near the truncated boundaries are positive, which is not physically correct. Using infinite elements eliminates this boundary effect. The use of infinite elements also improves the accuracy of the calculated maximum displacement by approximately 2%.

6.2 Elastic–plastic Solution

A model three-layered pavement structure is examined here. The geometric parameters and material properties are listed in Table I. Asphalt concrete is assumed to be elastic. The Drucker–Prager model, a constitutive model widely used for geotechnical materials, is used to describe base and subgrade materials. There are two parameters, the cohesion and the internal friction angle, in the Drucker–Prager model. A uniform $0.4\,\text{m} \times 0.4\,\text{m}$ square load of

TABLE I Structure parameters for the model problem

Layer	Thickness (m)	Material	Young's modulus (MPa)	Possion's ratio	Cohesion (MPa)	Internal friction angle
Surface	0.1	Elastic	1500	0.45		
Base	0.2	Elastic–plastic	200	0.3	0.690	20
Subgrade	3.7	Elastic–plastic	30	0.4	0.276	10

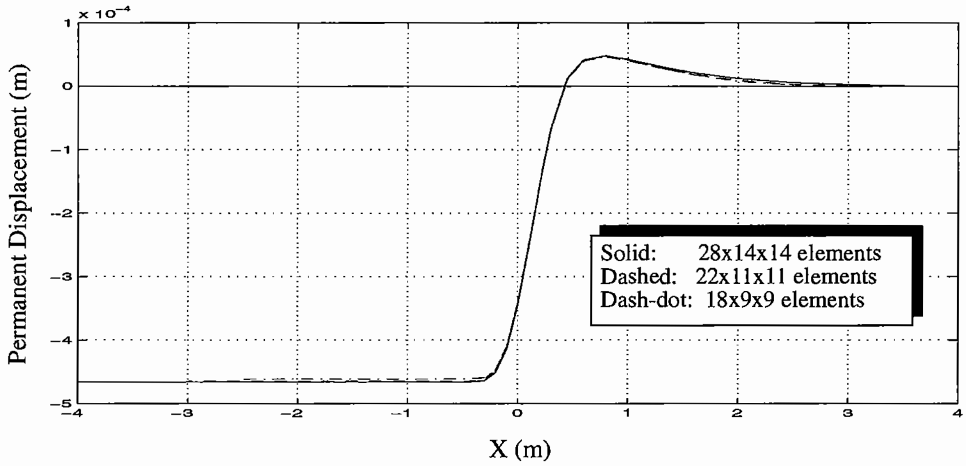

FIGURE 7 Results using infinite elements with different meshes.

0.8 MPa is applied to the surface of the pavement, which simulates the loading of a truck wheel.

A total of 28×14×14 elements are used in the finite element mesh, which represents a truncated domain of 8 m×4 m×4 m, in the x_1, x_2, and x_3 directions, respectively. The elastic results using this mesh are checked with theoretical solutions and the error of the maximum displacement is within 4% without using infinite elements and within 2% using infinite elements.

Figure 5 shows the displacement profile along the centerline of the pavement. Positive displacements are observed near the truncated boundary ahead of the load. This boundary effect is eliminated by using infinite elements.

Figure 6 is the vertical permanent displacement profile along the centerline of the pavement surface calculated from Eq. (32). Instead of giving a horizontal line behind the load as expected, the use of roller boundary conditions gives a curve, which decreases near the truncated boundary. The boundary effect is so obvious that it is almost impossible to estimate the residual vertical displacement. The introduction of the infinite elements and the modified iterative scheme completely eliminates this boundary effect and makes it easy to evaluate the residual displacement.

Two smaller meshes using infinite elements are also used in this model problem. One uses 22×11×11 elements with a truncated domain of 6 m×3 m×3 m; the other uses. 18×9×9 elements with a truncated domain of 5 m×2.5 m×2.5 m. The results are given in Fig. 7. These three meshes give almost the same residual displacements. This suggests that the adoption of infinite elements along with the iterative scheme for imposing the non-linear infinity conditions can greatly reduce the amount of storage and calculation (more than 70% in the current problem). Numerical results have shown that even a smaller mesh can give a fairly good estimation of residual displacements, however, the error in the maximum displacement will increase.

The improvement in numerical efficiency by using infinite elements becomes more significant for higher load levels. Figure 8 shows the vertical permanent displacement along the centerline of the pavement surface versus load. Since it is difficult to estimate the permanent displacements using the finite element method with roller boundary conditions, as shown in Fig. 6, the relevant values used in Fig. 8 are only rough estimates. The result for higher loads is very poor using roller boundary conditions with the mesh of 28×14×14 elements. At higher load levels, the rate of increase in the calculated permanent displacement decreases, which is obviously incorrect. This is due to the fact that when the load is higher, the yield zone is bigger and a bigger truncated domain must be used. A bigger mesh of 40×19×14 elements is also used as a

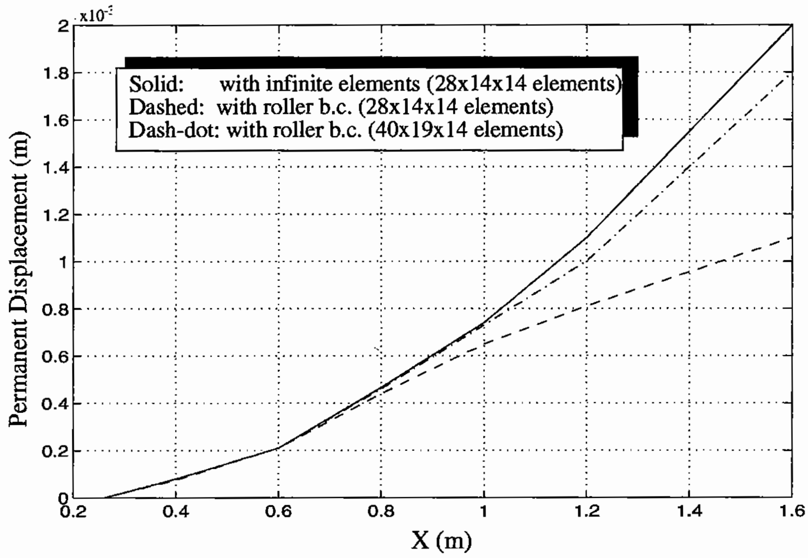

FIGURE 8 Permanent displacement versus load level.

comparison, which gives results similar to that using infinite elements but with only 28 × 14 × 14 elements.

Figure 9 gives the second deviatoric stress invariant (J_{2d}) in the lower half of the pavement surface along the centerline where the maximum tensile stress usually occurs. The curve indicates that the adoption of infinite elements has little effect on the stress state and residual stress state. This may be explained by the fact that the stresses behind the load converge to the residual stresses at a higher rate than the displacements converge to the residual displacements. Therefore, a relatively smaller mesh will give a good estimate of the residual stress state.

7. CONCLUSIONS

The geometrical, material and loading parameters used in the model problem are representative of most flexible pavement structures and load level they

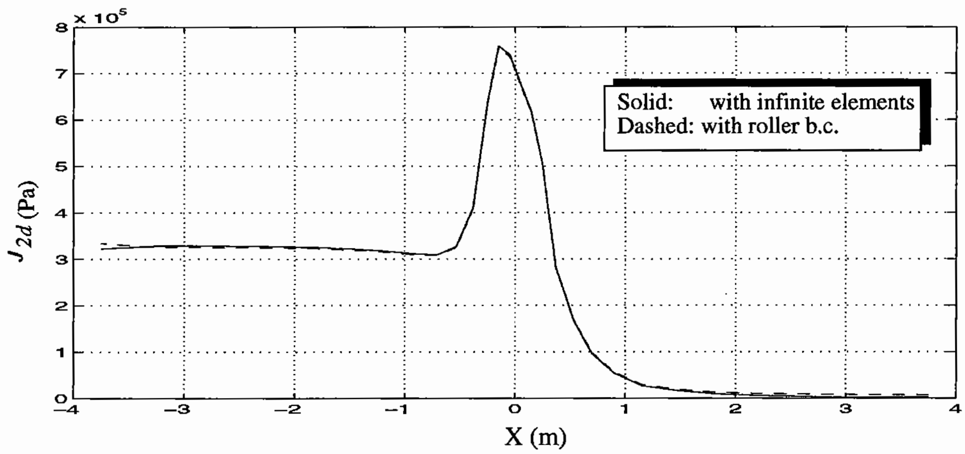

FIGURE 9 Stress state at the lower half of pavement surface.

experience. Based on the results obtained for this model problem, the following conclusions are drawn.

- Using infinite elements instead of roller boundary conditions improves the elastic solution for a halfspace.
- Using infinite elements along with the iterative scheme for imposing the non-linear infinity conditions also eliminates the boundary effects in the finite element algorithm for the problem of steady state moving loads on a layered elastic–plastic structure and gives a better prediction of the permanent deformations after the load has passed.
- This method greatly improves the results for high load levels, i.e. significant yielding. This suggests that problems such as wheel-wheel interaction, heavy aircraft loads or truck-load problems, which are difficult due to the large amount of computer storage and computing time, may be tractable with the adoption of infinite elements and the modified iterative scheme.
- The use of infinite elements has little effect on the residual stress state.

References

Bapat, C.N. and Batra, R.C. (1984) "Finite plane strain deformations of nonlinear viscoelastic rubber-covered rolls", *International Journal for Numerical Methods in Engineering* **20**, 1911–1927.

Bathe, K.-J. (1996) *Finite Element Procedures* (Prentice Hall, Englewood Cliffs, NJ).

Bhargava, V., Hahn, G.T. and Rubin, C.A. (1985) "An elastic–plastic finite element model of rolling contact", *Journal of Applied Mechanics* **52**, 75–82.

Dang Van, K. and Maitournam, M.H. (1993) "Steady-state flow in classical elasto-plasticity: applications to repeated rolling and sliding contact", *Journal of Mechanics and Physics of Solids* **41**, 1691–1710.

Desai, C.S. and Siriwardane, H.J. (1982) *Constitutive Laws for Engineering Media* (Prentice Hall, Englewood Cliffs, NJ).

Forte, T.K., Majizadeh, J.K., Hadden, J. and White, T. (1992) "Federal aviation administration pavement modeling", *Proceedings of Unified Airport Pavement Design and Analysis Concepts Workshop* DOT/FAA/RD-92/17, FAA, (US Department of Transporatation.

Ioannides, A.M. and Donnelly, J.P. (1992) "Development of user guidelines for a three-dimensional finite element pavement model", *Proceedings of Unified Airport Pavement Design and Analysis Concepts Workshop* DOT/FAA/RD-92/17, FAA, (US Department of Transportation.

Kirkner, D.J., Caulfield, P.N. and McCann, D.M. (1994) "Three-dimensional, finite-element simulation of permanent deformations in flexible systems", *Transportation Research Record* **1448**, 34–39.

Kirkner, D.J., Shen, W., Hammons, M.I. and Smith, D.M. (1996) "Numerical simulation of permanent deformation in flexible pavement systems subjected to moving loads", *Proceedings of the 11th Engineering Mechanics Conference* (American Society of Civil Engineers, pp. 430–433, p 433.

Kokkins, S.J. (1992) "FAA unified pavement analysis 3-D finite element method", *Proceedings of Unified Airport Pavement Design and Analysis Concepts Workshop* DOT/FAA/RD-92/17, FAA, (US Department of Transportation.

Lynch, F. (1969) "A finite element method of viscoelastic stress analysis with application to rolling contact problems, International", *Journal for Numerical Methods in Engineering*, 1.

Siriwardane, H.J. and Desai, C.S. (1983) "Computational procedures for non-linear three-dimensional analysis with some advanced constitutive laws", *International Journal of Numerical and Analytical Methods in Geomechanics* **7**, 143–171.

Zaghloul, S. and White, T. (1993) "Use of a three-dimensional, dynamic finite element program for analysis of flexible pavement", *Transportation Research Record* **1388**, 60–69.

Zienkiewicz, O.C. and Taylor, R.L. (1989) *The Finite Element Method* (McGraw-Hill, UK) **Vol. 1**.